Soft Matter

2D Protein Arrays induce 3D invivo-like assemblies of cells

Journal:	*Soft Matter*
Manuscript ID:	SM-COM-10-2014-002278.R1
Article Type:	Communication
Date Submitted by the Author:	20-Dec-2014
Complete List of Authors:	Moreno-Flores, Susana; University of Natural Resources and Life Sciences, Vienna (former address), kuepcue, Seta; University of Natural Resources and Applied Life Sciences, Center for Nanobiotechnology

2D Protein Arrays induce 3D invivo-like assemblies of cells

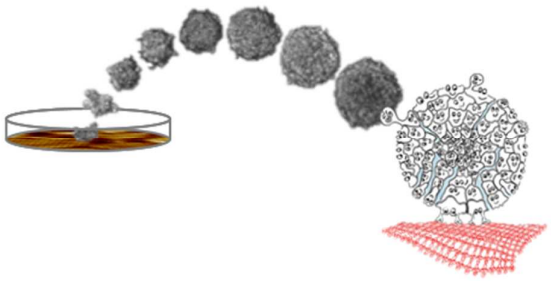

Bacterial S-layers trigger the formation of viable multicellular spheroids of adequate morphology, kinetics of growth and lifespan for biomedical research.

Journal Name

RSCPublishing

COMMUNICATION

2D Protein Arrays induce 3D invivo-like assemblies of cells

Cite this: DOI: 10.1039/x0xx00000x

S. Moreno-Flores[a] and S. Küpcü[b]

Received 00th January 2012,
Accepted 00th January 2012

DOI: 10.1039/x0xx00000x

www.rsc.org/

We report on the ability of two-dimensional protein crystals to induce the formation of homo- and heterotypic multicellular spheroids (MSCs) which resemble the morphology and hierarchical organization of living tissues and tumours. We have systematically studied the influence of the initial cell density and incubation time on the kinetics of spheroid growth and spheroid lifespan. Hereby a novel methodology has been established to produce MCSs on protein-based molecular layers.

Multicellular spheroids (MCSs) are spherical clusters of mammalian cells characterized by a complex 3D network of cell-cell and cell-matrix interactions (figure 1a)[1,2,3]. Made *in vitro*[4,5], MCSs are becoming the synthetic analogues of avascular *in vivo* tissues and tumours: they are not only morphologically similar but also behave alike to the diffusion of nutrients, oxygen, waste or therapeutic agents[6,7]. S-layers on the other hand are 2D protein arrays and major constituents of cell envelopes in many bacteria and archaea (figure 1b)[8,9,10]. Among them, the SbpA layer from *Lysinibacillus sphaericus* CCM 2177 displays a strong antifouling behaviour, hampering the adsorption of blood serum proteins when recrystallized on planar supports in biosensing devices[11] (figure 1c).

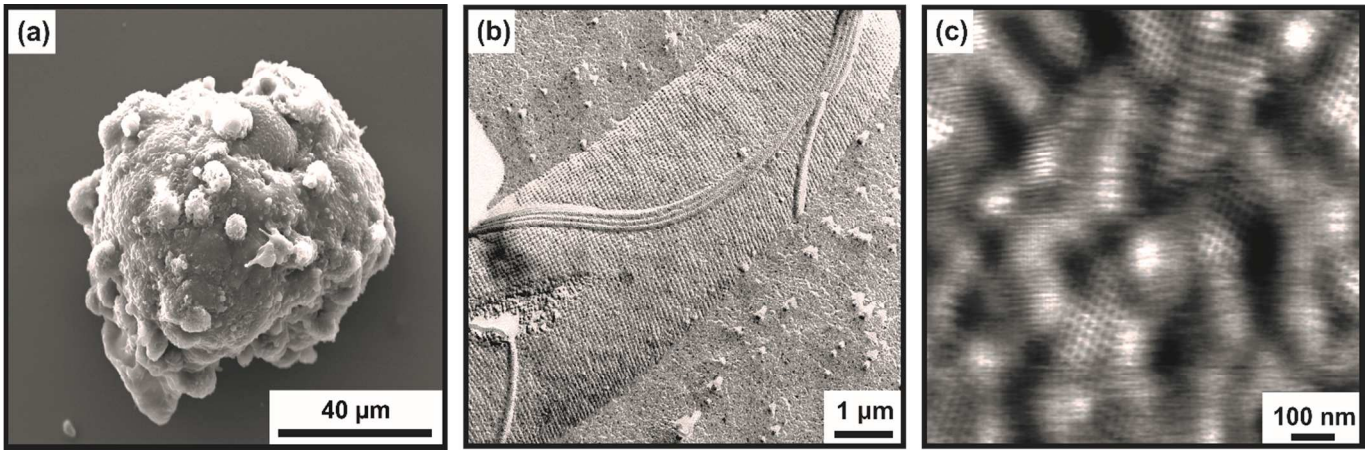

Figure 1. *Cell spheroids and S-layers*. a) Scanning electron micrograph of a single MCS of approximately 80 µm diameter (b) Electron micrograph of a freeze-etched preparation, showing the cell envelope of *Lysinibacillus sphaericus* CCM 2177 and the square-symmetric (p4) SbpA layer. (c) Atomic force micrograph of a recrystallized SbpA layer on glass.

Journal Name RSCPublishing

COMMUNICATION

Here we show that SbpA layers can induce the formation of MCSs beyond their recognised role as antifouling agents. By employing S-layers as substrates and a gradient of cell densities, we have produced MCSs and studied the influence of the initial cell number on their growth rate, shape and viable lifespan. This work presents a very simple method to produce homo- and heterotypic MCSs that merely requires the most elementary procedures of tissue culture and surface modification.

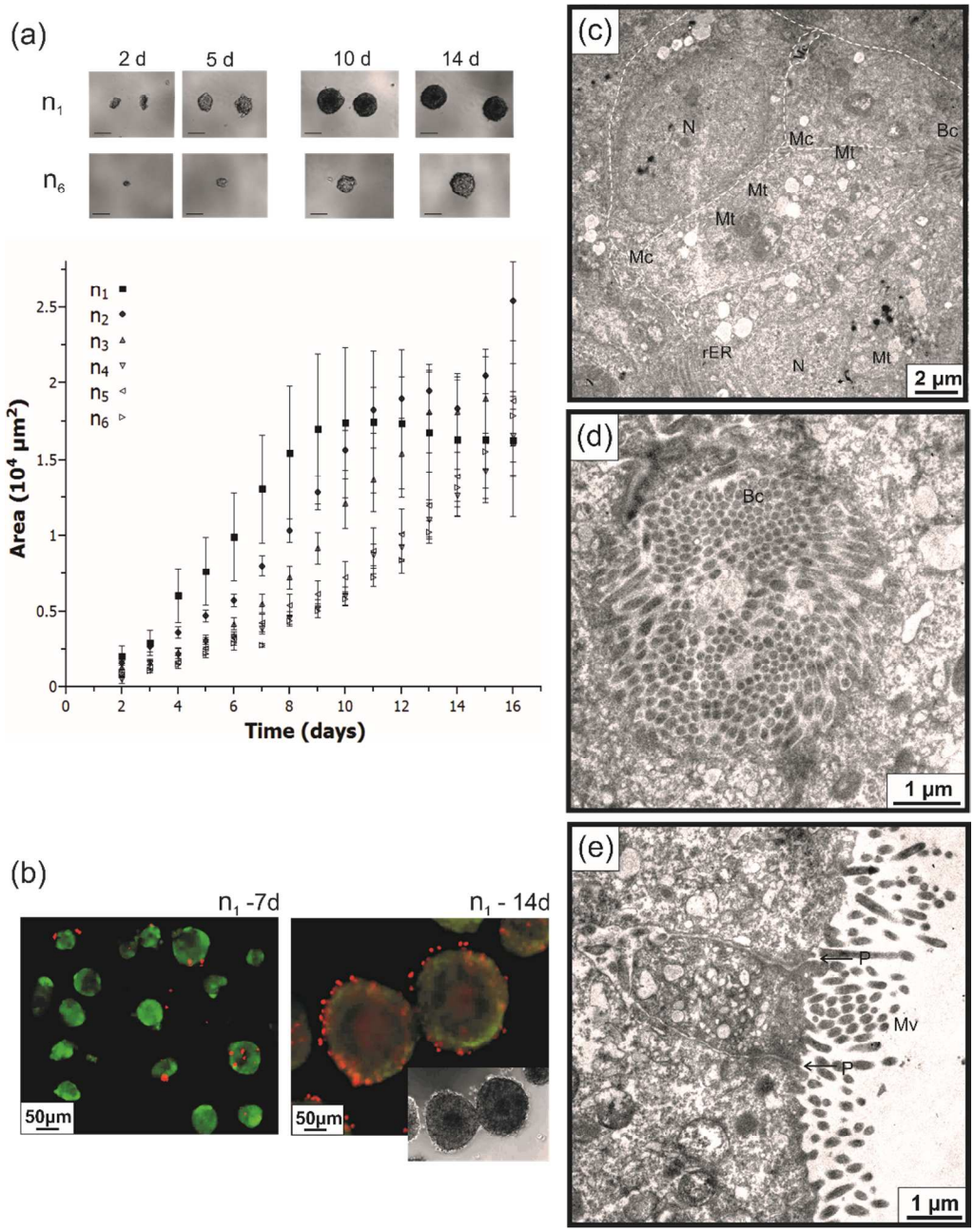

Figure 2. Formation of MCSs of HepG2 cells on SbpA layers. a) PhC optical micrographs of MCSs at different stages of spheroid development (2, 5 10 and 14 days of incubation) (scale bar = 100 µm). The graph below shows the projected area of an average MCS as a function of incubation time for the whole gradient of cell densities (n_1-n_6). b) Spheroid viability. Fluorescence micrographs of a live(green)-dead(red) assay on MCSs after 7 and 14 days of incubation. The inset is the corresponding PhC image, showing the dark cores in both MCSs.(c-e) Ultrastructure of MCSs of HepG2 cells as revealed by transmission

electron microscopy. Images of thin sections of a viable spheroid after 7 days of incubation (n_2): (c) Inner structure of close-packed cells, cells are outlined for the sake of clarity. (d) Inner structure of a bile canaliculi. A magnified view of an intercellular space filled with microvilli. (e) Outer structure of peripheral cells exhibiting a polarized structure of an apical surface with a high number of microvilli. Pores are also visible. (Identifiable cell organelles und structures: nucleus (N), mitochondria (Mt), rough endoplasmic reticulum (rER), microvilli (Mv), microvillus lined channel (Mc) or bile canaliculi (Bc), spheroid pore (P)).

Figure 2a shows two time-lapse series of phase-contrast (PhC) micrographs at different stages of spheroid development for the highest (n_1) and the lowest (n_6) initial cell densities. In both cases, spheroids originate in small cell clusters. However, the number of cells and hence the size of these *spheroid nuclei* depends on the initial cell density. At high cell density (n_1) and before sedimentation occurs, aggregation of either single cells or small cell clusters must not be uncommon. This results in the early formation of non-spherical cell clusters at the second day of incubation. At low cell density however, spheroids generate from significantly smaller clusters containing few cells (2-4), which suggests that cell aggregation either scarcely occurs or does not occur at all. The spherical shape is in this case preserved at the earlier stages of spheroid development. At this point, the growth of the cluster is determined by the proliferation of its constituent cells. In all cases though, the optical contrast of the spheroids increases as growth proceeds, which suggests that not only does the spheroid size increase but also the spheroid density. However, spheroid growth is not constant and it finally stops; the graph in figure 2a shows the projected area of an average spheroid as a function of the incubation time for the whole gradient of cell densities n_1-n_6. As reported previously, the projected area of the cluster at the second day of incubation is significantly higher at n_1: the spheroid thus grows at a faster rate. At the 10th day of incubation however, the projected area levels off and growth of the now mature spheroid stops. At the plateau, the optical contrast of the spheroids reaches a maximum, the spheroids become mobile and display dark cores as observed in the n_1-PhC micrographs. Contrarily, the growth rate of the spheroids at the lowest cell densities (n_4-n_6) is so slow that the plateau is not reached, even after 16 days of incubation. Under these conditions the spheroids require longer times to reach maturity.

For the highest cell densities ($n_4 < n \leq n_1$) the kinetics of spheroid growth is dependent on the initial cell number. The higher the cell density the larger the extent of cell aggregation at short incubation times (< 2 days), which in turn generates larger cell clusters and speeds up spheroid growth. After a long incubation and as a consequence of the increase in mobility, the spheroids may eventually coalesce, which can be at times observed as a further increase in area beyond the plateau (for example the n_2-data of figure 2a). However, at low cell densities ($n_6 < n \leq n_4$) cell aggregation does not occur in such a large extent and spheroids mainly develop from either single cells or small cell clusters. The graph in figure 2a shows that the projected area of an average spheroid at these initial cell densities behaves similarly with time: under these conditions, the spheroid growth is no longer determined by the initial cell density but by the rate at which cells proliferate within the spheroid. The data of figure 2a suggest that MCSs growth is sigmoidal, and thus spheroids evolve as populations do. Since MCSs, like tumours, are populations of cells growing in a confined space where the availability of nutrients is limited, their growth can be modelled by a function of the type used to describe tumour growth[12]. The Gomp-ex model, a modification of the classical Gompertz model suitable for small tumours, has proved to fit well our data[13]. The Gomp-ex model predicts an initial exponential growth until the population reaches a critical size, S_c, at time t_c. At longer times, the population starts competing for resources, growth slows and finally stops at sufficiently long times.

$$S(t) = \begin{cases} S_0 exp(\alpha t), & t < t_c \\ S_c exp\left(\frac{\alpha}{\beta}\right) exp\left[-\frac{\alpha}{\beta} e^{-\beta(t-t_c)}\right], & t \geq t_c \end{cases}$$

Where α and β are parameters related to the proliferation of the cells in the non-competing and competing environments, respectively. Fitting results[13] show that t_c decreases with initial cell density from 14 days (n_6) to 6 days (n_1). As suggested previously, $\alpha = 0.21 \pm 0.01$ and $\beta = 0.3 \pm 0.1$ (both expressed in days^{-1}) do not depend on the initial cell density when $n_6 < n \leq n_4$.

The appearance of a dark core in old spheroids defines the spheroid lifespan and hence deserves commenting. Live-dead assays were performed on mature spheroids (n_1 after 7 incubation days) and on old spheroids (after 14 incubation days), and the results are shown in the fluorescence micrographs of figure 2b. While the mature spheroids appear in green and therefore viable, the core as well as cells at the periphery of old spheroids appear in red, an evidence of cell necrosis. Cell death in the core of old spheroids may be seen as a consequence of the increase in spheroid density. An ever-increasing number of cells in a confined space gradually retards the diffusion of nutrients, oxygen to the inner cells, which will eventually lead to cell starvation. This diffusive barrier may as well impede the release of waste, which tends to accumulate in the cells, poisoning them. Either way leads to cell death[14]. However, the presence of dead cells loosely attached at the edges of old spheroids must have another cause, which may be the gradual loss of nutrients of an aged culture medium. The rate at which cell medium ages, increases with the number of MCSs and hence cell death at the periphery can be delayed if the former are cultured at low initial cell densities: MCSs cultured at n_4 exhibit necrotic cores but fewer dead peripheral cells after 21 days in culture[15]. Replacing regularly the cell medium with fresh one may prevent cell death at the periphery in that nutrients are periodically supplied and cell waste removed. In addition, it may delay the appearance of necrotic cores since it maintains the osmolality and restores concentration gradients for diffusive transport. However, the exchange of media cannot prevent cell death at the core, since it does not eliminate the diffusive barrier of a growing population of assembled cells[16] without the capacity of vascularize their structure. Consequently, spheroid viability is irremediably lost either in the core when the spheroids' size reaches a threshold value (>100 μm according to our studies[17]), or in the periphery under insufficiently nourishing conditions. In both cases cell death occurs at very long incubation times and therefore we can discard the bacterial S-layer as likely cause of loss in spheroid viability.

The inner structure of a mature MCS of viable HepG2 cells grown under these conditions, consists of closely-packed cells and microsized channels (figure 2c). Tubular projections of cell membrane, or microvilli (Mv), extend into these channels, as expected of this type of cells[18]. The channels are denoted as microvilli-lined channels (Mc) or bile canaliculi (Bc, figure 2d)[19]. Inner cells thus display structural polarity, depending on whether they are in close association with other cells or lining the bile canaliculi. In the latter case, cells develop a basal-apical polarity where the apical surface is comprised of microvilli, very much resembling the liver tissue. Cell basal-apical polarity also occurs at the spheroid surface. The transmission electron micrograph of figure 2e shows that at the microscale the surface of the MCS is not smooth, contrary to what has been previously reported[19]. Cells at the periphery arrange in a similar way as in the epithelial tissue, with

microvilli extending out of their apical surface and tightly bound to adjacent cells through their lateral surface. Figure 2e also shows the presence of pores (P), which have been hypothesized to open into the inner bile canaliculi and therefore provide a communication route between the inside of the spheroid and the surroundings[19].
So far it has been shown that the SbpA layer behaves as a biocompatible substrate in so much as it favours the development of homotypic MCSs over long periods of time[20]. In addition, the S-layer favours the self-assembly of co-cultured cell types to form spheroids with a defined core-shell structure. The formation of heterotypic associations is essential for the development of natural tissue, in particular the hepatic tissue: the *in vivo* liver is both structurally and functionally a heterocellular organ, and several *in vitro* studies have demonstrated that mixed cultures of primary hepatocytes with non-parenchymal cells such as fibroblasts or endothelial cells maintain hepatocyte viability and function[21,22,23]. When hepatocytes and fibroblasts are co-cultured on SbpA layers, the resulting spheroids exhibit a core of hepatocytes surrounded by a shell of fibroblasts (figure 3a)[24].

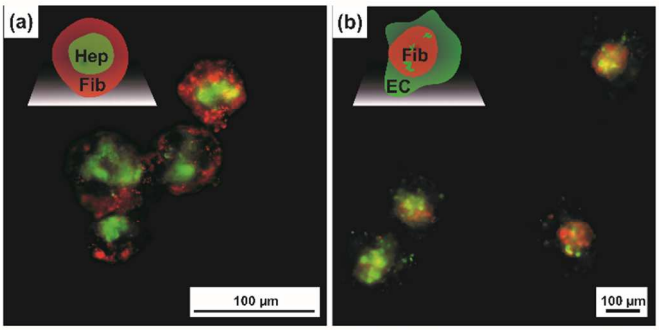

Figure 3. 3D co-culture on SbpA layers. a) Mixed spheroids showing a core of hepatocyte cells (Hep, green) surrounded by a shell of fibroblasts (Fib, red) after 5 days of incubation. b) Mixed spheroids with a fibroblast core (Fib, red) and a shell of HUVEC cells (EC, green) after 5 days of incubation.

Self-organization into core-shell spheroids maximises the heterotypic interface between the hepatocytes and fibroblasts, which has been reported to improve both the hepatocellular structure and function under *in vitro* conditions[21].
A similar type of cellular self-assembly has been observed for the first time in mixed cultures of fibroblasts and endothelial cells on SbpA layers (figure 3b). In this case, fibroblasts (in red) form sphere-like aggregates surrounded by an uneven distribution of endothelial cells, (EC, in green) Although we cannot exclude the possibility of EC migration into the fibroblast core based on the location and distribution of the fluorescence intensity, figure 3b shows heterotypic MCSs with compact fibroblast cores and diffused EC shells., a cellular arrangement that resembles the *in vivo* structure of non-parenchymal tissue. Fibroblasts are the cellular components of connective tissue that binds, protects and supports other tissues or organs in the body. The connective tissue has no free surface and it is usually lined with a layer or layers of either endothelial or epithelial cells. Each MCS of figure 3b is an enclosed micro model of the heterocellular structure lining blood vessels and organ cavities. Such a spheroid can provide a controlled and confined environment to study angiogenesis, the extravascular migration of lymphocytes (inflammation), cancerous cells or drugs and simulate the first stages of the immunological response, drug delivery or metastasis[25].
The ability of SbpA layers to promote or inhibit cell adhesion depends on the side of the layer that is exposed to the cells, which in turn depends on the pH at which recrystallization occurs[26]. At pH 9-9.5, the SbpA layer recrystallizes with its smooth, antifouling side up, which is also the side exposed to the medium in the native environment. Therefore it is called outer side. Compared to the inner side, the outer is flatter, has a negative zeta potential of approximately -50 mV in contrast to the inner side's +20 mV, and it is comprised of two protein monolayers, which are assembled one on top of the other with their inner sides facing each other[26]. This layer on the one hand inhibits both protein adsorption and cell adhesion in two-dimensional cultures; on the other hand, it induces the formation and development of three-dimensional cell spheroids. This means, the interaction between the SbpA layer and the cells does not promote cell spreading and growth in monolayers, however it allows cell anchoring in the early and intermediate stages of spheroid development[27]. Regardless of the nature of such interaction, which undoubtedly deserves further investigation, the reported study proves the suitability of the SbpA layer as a ready-to-use, biocompatible material for the production and maintenance of multicellular spheroids that display the appropriate morphology for an optimal cell-cell communication. In the specific case of carcinoma cells such as HepG2 and the heterotypic MCSs, whose cytokine release should be tested first for a possible immunoresponse to the SbpA layer[28], the method can be employed to generate targets for *insitu* and *exsitu* drug screening and chemo-, radio- or immunotherapy research or to provide models of heterotypic interactions to investigate *insitu*/*exsitu* tumour angiogenesis and metastasis.

Experimental.
Materials. Hepatocellular carcinoma cells (HepG2), normal human dermal fibroblasts (NHDFs) and human umbilical vein endothelial cells (HUVECs) were purchased from ATCC (LGC Standards GmbH, Wesel, Germany) Medium for tissue culture (DMEM) complemented with 10% fetal bovine serum (FBS, Gibco, USA), 1% GlutaMax™ (Life technologies, Thermo Fisher Scientific, USA) and 1% antibiotic/antimycotic solution (Sigma-Aldrich, Austria) were employed for both 2D and 3D tissue culture (TC). SbpA proteins were isolated from *Lysinibacillus sphaericus* CCM 2177 and subsequently purified as reported elsewhere[29]. The purified protein (1 mg/ml in water) diluted 1:10 in recrystallization buffer (0.5 mM Tris-(hydroxymethyl)aminomethane), 10 mM $CaCl_2$, pH=9-9.5) will be referred to as recrystallization solution.
Recrystallization of SbpA on TC plates. 100 µl of recrystallization solution were added to 96-well tissue culture plates (IWAKI, Japan) and incubated for longer than 12h at room temperature. The solution contains approximately a 240-fold excess of protein required to fully cover the bottom of the well with a defect-free monolayer. After incubation the plates were rinsed three times with Milli-Q water (Millipore, Austria) and filled with TC medium before cell seeding.
Cell & spheroid culture (homotypic cultures). Cells for spheroid production were obtained from monolayer cultures at 80% confluence. After being rinsed with phosphate buffer (PBS) and treated with Trypsin/EDTA (PAA, Austria, now GE Healthcare) at 37 °C for 3 min, the cell suspension was centrifuged at 12500 rpm for 5 min. The resulting pellet was resuspended in fresh TC medium and left for the largest cell aggregates to sediment. Viable one-to-three-cell suspensions were attained after approximately 20 minutes, during which optical inspection, cell counting and cell viability against Trypan Blue were carried out every 10 minutes (Countess, Invitrogen, USA). Cells were then seeded in a series of 96-well plates coated with SbpA by sequential 1:2 dilution to produce a gradient of cell densities[30].
Cell & spheroid culture (heterotypic cultures). NHDFs were co-cultured with either HepG2 cells or HUVECs. Previously, the cell

membranes were fluorescently labelled (PromoKine, Biomedica, Austria) according to the manufacturer's protocol. The ratio of NHDFs to HepG2 or HUVECs for 3D co-culture was chosen to be 1:2.5. Cells of both lines were first mixed at this ratio before being plated in SbpA-coated 96 well plates. Co-cultures were maintained in DMEM medium.

Optical microscopy. Spheroid growth was monitored as a function of the incubation time with an inverted fluorescence optical microscope (TE2000, Nikon, Japan) equipped with a digital camera (DS-Qi1MC, Nikon). Low resolution, phase-contrast micrographs of each well were acquired once every 24 hours approximately for a total of 16 days.

Image analysis. Optical micrographs were analysed with an image processing and analysis freeware (ImageJ, National Institutes of Health, USA). The graphs of figure 2 display the data averages from images of sample triplicates at a specific incubation time.

Live-dead assays. Spheroid viability was qualitatively evaluated after 7 and 14 days of incubation using a commercially available fluorescence assay (LIVE/DEAD® Viability/Cytotoxicity Assay, Life Technologies, Austria).

Electron microscopy. Homotypic spheroids were fixed with 1% tannic acid (Fluka, Austria) in a glutaraldehyde-formaldehyde fixative solution[31] overnight at 4°C.

Transmission electron microscopy. After fixation the spheroids were embedded in 1% agarose and prepared for observation as previously reported[32]. The resulting ultrathin sections were observed with a transmission electron microscope (FEI Tecnai G^2 20, FEI Europe, Netherlands) operating at 120 kV. Images were acquired with an FEI Eagle 4K camera.

Scanning electron microscopy. Fixed spheroids were first dehydrated by sequential 10 min-immersion in a gradient of ethanol (50, 70, 80, 90, 95 and 100%), followed by 50% hexamethyldisilazane (HMDS, Fluka, Austria), before overnight immersion in 100% HMDS. The dried samples were then mounted on aluminium stabs and sputter-coated with a 5 nm layer of gold (EMSC005, Leica, Germany). Samples were observed with a scanning electron microscope (FEI Inspect S50, FEI Europe, Netherlands) operating at 5 kV.

Conclusions

Bacterial SbpA layers are suitable supports for three-dimensional cell culture, allowing the formation and growth of multicellular spheroids for lengthy periods of time. Mature MCSs made of HepG2 cells exhibit a typical tissue-like structure of polarized cells, pores and channels, which evidences an effective intercellular communication and viability. Heterotypic MCSs show a singular core-shell morphology that resembles the in vivo scenario of adjacent tissues. Since these types of MCSs prove most appropriate micromodels of tissular organization and cell communication, this work has implications in that it implicitly outlines a simple, ready-to-use, throughput-tunable methodology to produce viable MCSs with potential biomedical applications in tumour research, including tumour invasion and therapy design, as well as in tissue and organ reconstruction.

Acknowledgments

The authors would like to thank Andrea Scheberl and Mario Rothbauer for their assistance in the experiments of thin section-transmission electron microscopy and scanning electron microscopy, respectively. Special thanks to Eva-Kathrin Sinner for her support and also to Maria dM Vivanco for their comments on the manuscript.

Notes and references

[a] University of Natural Resources and Life Sciences, Vienna, 1190 Vienna, Austria (former address). Email: smf8097@gmail.com.

[b] Institute of Synthetic Bioarchitectures, Department of Nanobiotechnology, University of Natural Resources and Life Sciences, Vienna, Muthgasse 11, 1190 Vienna, Austria. Email: seta.kuepcue@boku.ac.at

Electronic Supplementary Information (ESI) available in a separate file (supp info.pdf) See DOI: 10.1039/c000000x/

1 J. Holtfreter, *J. Exp. Zool.* 2006, **95**, 171.
2 A. Moscona and H. Moscona, *J. Anat.* 1952, **86**, 287.
3 R. M. Sutherland, *Science* 1988, **240**, 177.
4 R.-Z. Lin and H.-Y. Chang, *Biotechnol. J.* 2008, **3**, 1172.
5 X. Li, A.V. Valadez, P. Zuo and Z. Nie, *Bioanalysis* 2012, **4**, 1509.
6 C. Dubessy, J. M. Merlin, C. Marchal and F. Guillemin, *Crit. Rev. Oncol. Hematol.* 2000, **36**, 179.
7 H.-L. Ma, Q. Jiang, S. Han, Y. Wu, J. C. Tomshine, D. Wang, Y. Gan, G. Zou and X.-Y. Liang, *Molecular Imaging* 2012, **11**, 487.
8 U. B. Sleytr, *Int. Rev. Cytol.* 1978, **53**, 1.
9 U. B. Sleytr, and T. J. Beveridge, *Trends Microbiol.* 1999, **7**, 253.
10 M. Sára and U. B. Sleytr, *J. Bacteriol.* 2000, **182**, 859.
11 M. M. Picher, S. Küpcü, C. Huang, D. Dostalek, D. Pum and U. B. Sleytr, P. Ertl, *Lab chip* 2013, **13**, 1780.
12 M. Marušic, Ž. Bajzert, J. P. Freyer and S. Vuk-Pavlović, *Cell Prolif.* 1994, **27**, 73.
13 For details about the Gomp-ex model and related literature, the authors refer to the supporting information, figures S3 and S4.
14 E. Curcio, S. Saleerno, G. Barbieri, L. De Bartol, E. Drioli and A. Bader, *Bioanalysis* 2007, **28**, 5487.
15 The authors refer to the figure S5 of the supporting information.
16 M. Divr-Ginzberg, T. Elkayam, E.D. Aflalo, R. Abgaria and S. Cohen, *Tissue Engineering* 2004, **10**, 1806.
17 The authors refer to the supporting information, figures S5 and S6.
18 HepG2 are hepatocytes, which are epithelial in morphology. D. The´ard, M. Steiner, D. Kalicharan, D. Hoekstra, S.C.D. van IJzendoon, *Mol. Biol. Cell* 2007, **18**, 2313.
19 S. F. Abu-Absi, J. R. Friend, L. K. Hansen and W.-S. Hu, *Exp. Cell Res*. 2002, **274**, 56.
20 For additional examples of MCSs made of cells other than HepG2, the authors refer to figure S1 of the supporting information.
21 S. N. Bathia, U. J. Balis, M. L. Yarmush and M. Toner, *FASEB J.* 1999, **13**, 1883.
22 S. F.Abu-Absi, L. K. Hansen and W.S. Hu, *Cytotechnology* 2004, **45**, 125.
23 C. H. Cho, J. Park, A. W. Tilles, F. Berthiaume, M. Toner and M. Yarmush. *BioTechniques* 2010, **48**, 47.

24 The resulting spheroids are viable, with few dead cells randomly distributed. The authors refer to the supporting information, figure S7.
25 L. A. Kunz-Schughart, J. A. Schroeder, M. Wondrak, F. van Rey, K. Lehla, F. Hofstaedter and D. N. Wheatley, *Am J Physiol Cell Physiol* 2006, **290**, 1385.
26 M. Rothbauer, S. Küpcü, D. Sticker, U. B. Sleytr and P. Ertl, *ACSNano* 2013, **7**, 8020.
27 Young and mature spheroids remain in the same position for days. Gentle movement during sample handling or gentle pipetting of TC medium do not alter the spheroids´ position. Shear flow however, such as that employed in microfluidic experiments flushes the spheroids away.
28 B. Jahn-Schmid, U. Siemann, A. Zenker, B.Bohle, P. Messner, F. M. Unger, U. B. Sleytr, O. Scheiner and D. Kraft, *International Immunology* 1997, **9**, 1867.
29 U. B. Sleytr, M. Sára, Z. Küpcü and P. Messner, *Arch. Microbiol.* 1986, **146**, 19.
30 For details of the production of the cell density gradient the authors refer to the supporting information
31 A. M. Glauert and P. R. Lewis, *Biological sample preparation for Transmission Electron Microscopy,* Portland Press, London, 1st edn., 1998, ch 2, 21-75
32 M. H. Ücisik, S. Küpcü, M. Debreczeny, B. Schuster, U. B. Sleytr, *Small* 2013, **9**, 2895.

